



Thin film thermocouple fabrication and its application for real-time temperature measurement inside PEMFC

Yu-Qing Tang^a, Wen-Zhen Fang^{a,b}, Hong Lin^a, Wen-Quan Tao^{a,*}

^a Key Laboratory of Thermo-Fluid Science and Engineering of MOE, School of Energy and Power Engineering, Xi'an Jiaotong University, Xi'an, Shaanxi 710049, China

^b School of Mechanical and Aerospace Engineering, Nanyang Technological University, Singapore 639798, Singapore

ARTICLE INFO

Article history:

Received 10 May 2019

Received in revised form 7 July 2019

Accepted 8 July 2019

Available online 17 July 2019

Keywords:

PEMFC

MEMS

Thin film thermocouple

Real-time temperature measurement

ABSTRACT

Temperature distribution in proton exchange membrane fuel cell (PEMFC) is of great importance to water and thermal management. In this study, 25 μm thick Type-T thin film thermocouples (TFTCs) were fabricated using micro-electro-mechanical system (MEMS) to realize the real-time measurement of temperature distribution inside PEMFC. Besides, fifteen sheathed thermocouples were used to measure the temperature distribution outside the cell. The effect of inserting TFTCs on the cell performance was confirmed to be negligible. The experimental results show that the embedded TFTCs can rapidly response to temperature regime while have a minimal interference to the performance of the fuel cell. The temperature variation of the inside TFTCs with current generally has the same trend with the outside sheathed thermocouples, but with a more frequent fluctuation due to their small thermal inertia and inside complex environment. In this work, the details of MEMS-based techniques of making TFTCs and measured distribution of inside cell temperature are provided.

© 2019 Published by Elsevier Ltd.

1. Introduction

In recent decades, the proton exchange membrane fuel cells (PEMFCs) have extensively developed due to its low operating temperature ($T < 120\text{ }^\circ\text{C}$), high energy efficiency, no pollution, little noise, and higher energy density compared with other conventional systems [1–3]. However, several issues such as cost and lifetime are the main barriers for the wide commercialization of fuel cells and other batteries [4,5]. Among the factors that affect the cost and lifetime of PEMFCs, thermal management is a major concern [6,7]. On one hand, too low temperature will affect the activity of catalyst, and can even lead to water flooding in the cathode. On the other hand, too high temperature can lead to the dehydration of the membrane, and further the performance degradation of the PEMFC [8].

As mentioned above, the temperature regime is of significance to the working performance of the PEMFC, especially for the cathode membrane electrode assembly (MEA) where most heat and water are produced [9,10]. Thus, the in-situ temperature measurement of the MEA is highly important to further reveal the characteristics of the internal process and to monitor the working conditions of the PEMFC.

Direct measurement of temperature is a widely adopted technique and has its advantages of simplicity and reliability. However, there is an inevitable interference to the object measured. In principle, the inevitable interference caused by temperature measurement should be controlled to a minimal level. Nevertheless, the scale of PEMFC along the film thickness direction is in millimeter and the measuring space is narrow and limited [11]. Thus, the traditional sensors are not suitable for the inside temperature measurement.

Recently, many efforts have been made to study on the real-time temperature measurement in a PEMFC. For example, Guo et al. [12,13] adopted the infrared imaging technology to measure the temperature distributions on the surface of the MEA with a self-designed PEMFC, which is an efficient way to measure the surface temperature field of fuel cells and cell stacks. However, it cannot reflect the interior temperature regime directly without changing the original structure of the cell since the inside infrared information cannot be detected by the sensor. Liu et al. [14] embedded four pairs of sensors into a fuel cell to measure the temperature and heat flux at the outer surface of the gas diffusion layer. Nevertheless, only one temperature sensor works well in the experiment and several significant parameters, such as the total thickness and wire width of sensor, were not mentioned in their work. Lee et al. [15–17] and Wang et al. [18] developed micro temperature sensors based on the principle of resistance tempera-

* Corresponding author.

E-mail address: wqtao@mail.xjtu.edu.cn (W.-Q. Tao).

ture detector by micro electro mechanical system (MEMS) technology. The microsensor they made was about $40\ \mu\text{m}$ in thickness with excellent strength which was suitable for the electrochemical environment and can be placed anywhere between the MEA and the flow channel. He et al. [19] developed a thin film gold thermistor for application in an operating fuel cell, which was embedded in parylene film laminated in the Nafion electrolyte layer using micro-fabrication techniques. However, the introduced double membrane will affect the accuracy and sensitivity of the microsensor. Besides, noble metals like gold were used at above studies that increases the fabrication cost. Sasaki et al [20] fabricated an in-line thermocouple of $49\ \mu\text{m}$ diameter to monitor the temperature along the through-plane direction, which can measure several spots simultaneously but takes lots of time to assemble the cell with the in-line thermocouples. Ali et al. [21] presented Type-T (copper-constantan) thin film thermocouples (TFTCs) array on a $75\ \mu\text{m}$ thick Kapton foil for measuring the inside temperature of high temperature PEMFC. Sugimoto et al. [22] measured temperature inside PEMFCs using Au-Ni TFTC array fabricated on parylene film, whose applications may be limited by the size of the cell since the TFTCs are presented by the form of array.

The previous studies have shown that thin film microsensor is a promising tool to in-situ measure the temperature distribution inside an operating cell due to their small size, high sensitivity and flexibility. Especially, it can reduce the inevitable interferences, such as the increase of the mass transfer resistance and electrical resistance, and can avoid the leakage of reactant gases when inserting sensors without refitting the original structure of the cell. Generally, ideal microsensors should have the following characteristics: (1) enough durability during assembling; (2) minimal size to reduce influence on the cell performance; (3) low cost, easy fabrication and high flexibility to achieve commercialization. To the authors' best knowledge, the previous developed microsensors do not possess the above characteristics simultaneously, either too large in thickness [20,21], or high cost in use of noble metal [15–19,22] and low flexibility [21,22]. In this paper, an embedded Type-T thin film thermocouple (TFTC) based on MEMS technology is developed to in-situ measure temperature variation and distribution of MEA inside the PEMFC. The total thickness of the TFTC is around $25\ \mu\text{m}$, with a polyimide (PI) film as the bottom isolating layer due to its excellent stability and high glass transition temperature in the vicinity of $400\ ^\circ\text{C}$ [23]. Such microsensor is made of cheap metals to save the manufacturing cost, and it has the advantages of small size, high sensitivity and flexibility.

The rest of the paper is organized as follows. The detailed processes of TFTCs design, fabrication and calibration are introduced in Section 2. The application of the TFTCs for PEMFC and experimental system of PEMFC are shown in Section 3. The real-time temperature measurement and detailed temperature variations and distribution inside the PEMFC are discussed in Section 4. Finally, several conclusions are drawn in Section 5.

2. TFTCs design, fabrication and calibration

2.1. TFTCs design

TFTCs were designed on a 4-in. PI film ($25\ \mu\text{m}$ in thickness) by MEMS fabrication techniques. Type-T TFTCs were selected in the present study due to their accuracy, low cost and fairly high Seebeck coefficient relative to other thermocouple types [24]. Type-T thermocouple yields excellent linearity within the temperature range of $-70\ ^\circ\text{C}$ to $400\ ^\circ\text{C}$, which is appropriate for the working temperature range of PEMFC. In addition, according to the theory of Seebeck effect, the thermoelectric potential output from thermocouple is only the function of temperature difference between

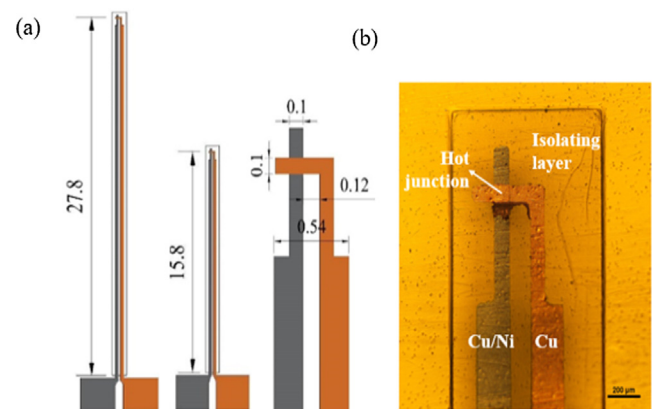


Fig. 1. (a) TFTC design layout. (Unit: mm). (b) Micrograph of TFTC.

two ends, which is not affected by pressure. Fig. 1(a) presents the design layout of TFTC, the region in gray color represents the deposited material of constantan material and the yellow color¹ represents the material of copper. Among the designed fourteen TFTCs, there are six long TFTCs and eight short TFTCs for the various sites of measurement, with the length of 27.8 mm and 15.8 mm, respectively. The metal junction area of TFTC is $100\ \mu\text{m} \times 100\ \mu\text{m}$ that has enough small spatial resolution for the temperature distribution inside the cell. The smaller size of junction area could benefit the performance of the sensor, however it may arise the durability issues. Thus, junction size in $100 \times 100\ \mu\text{m}$ is chosen. The junction dimension can be designed based on the photomask. A photolithography procedure is adopted to transfer the pattern on the photomask to the film substrate with a high degree of precision. The width of the TFTC sensor at the tail part increases to be $210\ \mu\text{m}$ (as shown in Fig. 1(a)) to enhance the wire strength. The micrograph of the fabricated TFTC is shown in Fig. 1(b). From the figure the two thermal electrodes, hot junction and isolating layer can be clearly observed, which match the design layout very well.

2.2. TFTCs fabrication

Following the designed pattern, TFTCs were fabricated according to an integrated technological process. The fabrication sequence of the TFTCs is shown in Fig. 2: (a) The PI film substrate was immersed in acetone and then vibrated by ultrasonic cleaner for 3 min to remove surface oil and fine dust; The clean PI film was put on the hot plate ($110\ ^\circ\text{C}$, 5 min) to dry the PI film surface after blowing. (b) Before coating the photoresist, plasma etching was employed to the surface of the PI film for 4 min. The main purpose of this plasma etching was to improve the adhesion between photoresist and PI film surface. The photoresist AZ5214 was coated and patterned by photolithography. (c) The layer of constantan was deposited by magnetron sputter after improving metal adhesion to PI film surface by O_2 plasma for 2 min, and then (d) constantan layer was patterned via lift off method. (e) The patterns of copper layer on the mask was transferred to the photoresist layer by lithography. (f) The layer of copper was deposited by e-beam evaporator also after O_2 plasma treatment. (g) Copper layer was patterned by lift off. (h) The photoresist AZ4620 was coated as a top insulation layer, which also protected the surface of the Type-T TFTCs against the harsh electrochemical environment inside the fuel cell. The spin coating process was performed at 6000 rpm for 30 s. Finally, the signal pins of the TFTC were exposed by pho-

¹ For interpretation of color in Figs. 1 and 7, the reader is referred to the web version of this article.

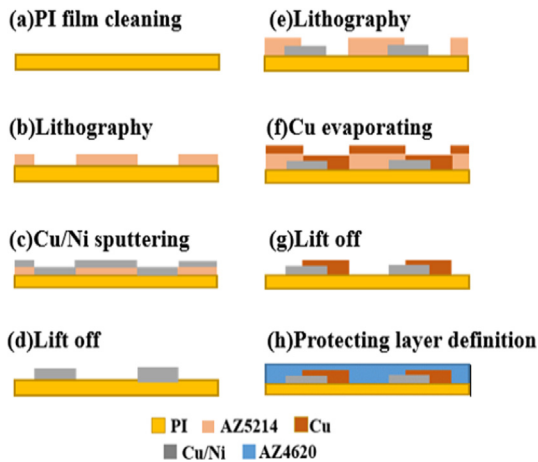


Fig. 2. Fabrication flowchart of TFTCs.

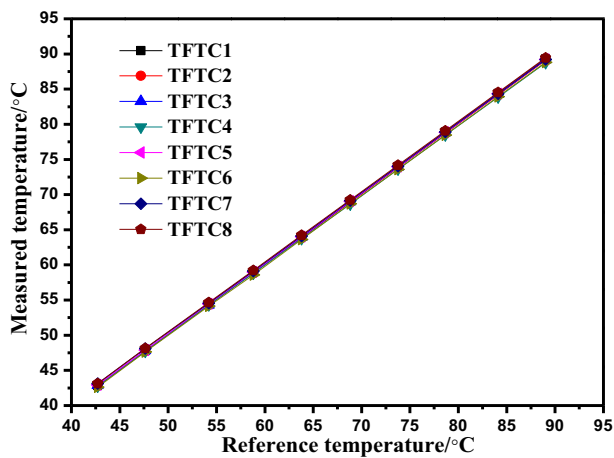


Fig. 3. Calibration curves of TFTCs.

tolithography for the signal output of thermoelectric potential. After the photolithography process, the sample was cured for half an hour at 110 °C.

2.3. TFTCs calibration

The homemade thermocouple is not a standard temperature sensor, and it must be calibrated before using it to measure the temperature. The calibration test was performed in a programmable temperature chamber. The TFC signal pins are connected to printed circuit board using Cu and Cu/Ni wires. The wires were also used between the printed circuit board and a data logger (Keithley). TFTCs assembly along with a reference thermometer (PT100) were placed in the chamber and calibrated from 45 °C to 90 °C with an interval of 5 °C. Once the temperature reached the set value and stay steady, the calibration data were output from Keithley to computer. The calibration curves of No.1 TFC to No.8 TFC can be seen in Fig. 3. Table 1 shows the linearity values of eight TFTCs. The results show that the micro temperature sensor has the good linearity and repeatability. The closer the values of R^2 to 1, the better the linearity of the sensors.

Table 1
Linearity values of TFTCs.

TFTCs	TFTC1	TFTC2	TFTC3	TFTC4	TFTC5	TFTC6	TFTC7	TFTC8
R^2	1	0.99999	0.99998	0.99995	0.99998	0.99993	0.99997	0.99998

2.4. TFTCs embedding

The TFTCs were put between the flow field plate and MEA for the inside temperature distribution measurement. They were numbered from No.1 to No.8, as shown in Fig. 4(a). Importantly, Teflon seals should be adopted to prevent the reaction gases escaping. The dimensions of two backing plates are 12 cm × 12 cm × 2 cm, and anode backing plate have 15 perforated holes to insert the sheathed thermocouples, as shown in Fig. 4(b). In the present study, the temperature distribution of anode current collector plate (ACCP) was measured using 15 sheathed thermocouples for which the details can be seen in our previous study [25].

After each part had been installed, the PEMFC was assembled through eight M6 screws with a uniform torque of 2 N·m. To control the working temperature of PEMFC, eight heating rods in total each with power of 30 W were inserted into the end plates of cathode and anode equally and two system-provided thermocouples were used to determine the temperatures of the two end plates. In this study, the temperature determined by system-provided thermocouples is denoted as the cell temperature; the temperature measured by the TFTCs are named as the inside temperature; and the temperature measured by the sheathed thermocouples is named as the outside temperature. The positions of all temperature sensors in a single cell are presented in Fig. 5.

3. Experimental method

3.1. The experimental system

The real-time inside PEMFC process measurement was conducted on the Arbin fuel cell testing system. This system is composed of several subsystems, such as flow/temperature/pressure module, gas handling module, humidifier module and electronic load [26]; the customized Arbin testing system can monitor and control the gas supply, the temperature of the cell and electronic load. The performance evaluation test was carried out in a 50 cm² single fuel cell using graphite flow plates with parallel channels. The depth of the flow channels is 1 mm, and the width of the channels and ribs are both 1.16 mm. The membrane electrode assembly (MEA) is SFR7201, and Pt loading amount in the MEA is 0.5 mg/cm².

3.2. Measurement procedure

The fuel cell performance is usually evaluated by current-voltage behaviors. Potentiostatic and galvanostatic are the two common modes to control the cell output of voltage or current [27]. The potentiostatic mode was adopted in the present study. The main procedures of the fuel cell performance test and temperature measurement are described as follows:

First, establish the initial steady state of this measuring process, which usually takes about one hour. In this work, the gas flow rate is constant and the stoichiometric ratios in the cathode and anode were 3 and 1.5, respectively at the initial temperature and current density of 1 A/cm². The inlet relative humidities of oxygen and hydrogen were set to be 25% and 100%, respectively. Other detailed initial conditions are listed in Table 2. Before reaching the required conditions, all parameters, such as gas temperature, humidifier temperature, cell temperature of two backing plates and gas flow rates, were carefully monitored under open circuit voltage

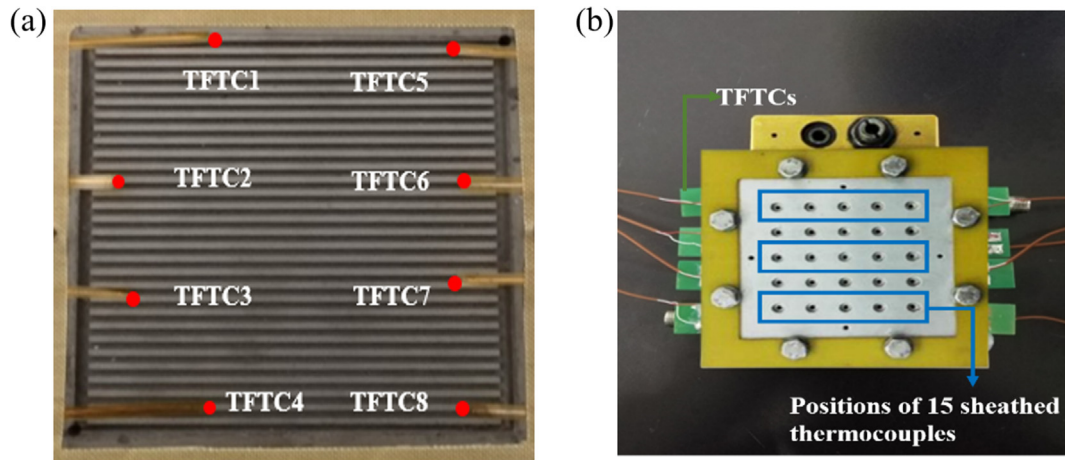


Fig. 4. (a) Measuring positions of embedded TFTCs. (b) Single cell with TFTCs and positions of 15 sheathed thermocouples.

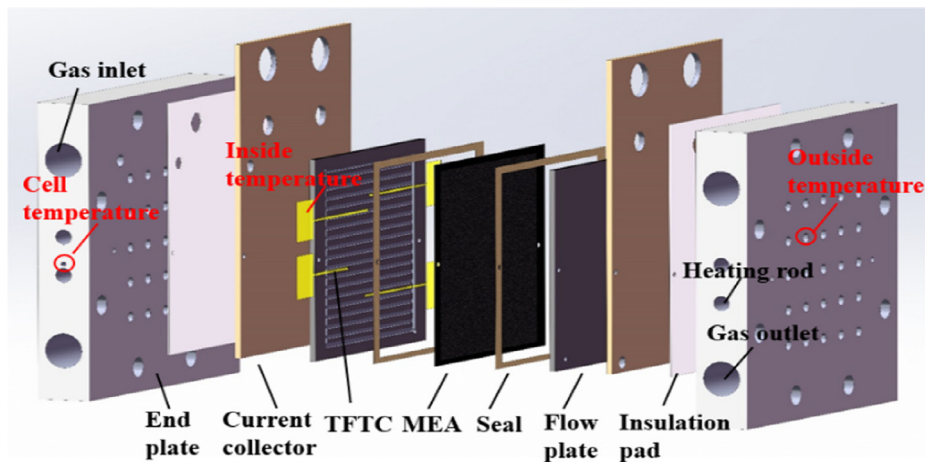


Fig. 5. The positions of the system-provided temperature sensors (cell temperature), TFTC (inside temperature), and sheathed thermocouples (outside temperature) in a single cell.

conditions. The eight heating rods were used to keep the required backing plate temperature.

Second, diminish the effects of loading history. The previous experiments under different working conditions would bring unexpected influences into the test. In accordance with the method adopted by Tajiri et al. [29], the tested cell was kept constant current density of 0.4 A/cm^2 for one hour to diminish the effects of the loading history.

Third, use potentiostatic modes to determine current-voltage behaviors. In this mode, current density was measured at constant voltage set from 0.9 V to 0.3 V with an interval of 0.1 V . Fig. 6 compares the performance curves of the fuel cell embedded with and without TFTCs, which were tested individually under the same working conditions. The embedded TFTCs in the cell will reduce the electrically conductive area or cover the area of MEA that prevents the reactant gas from diffusing through this area, leading to some degradation of power density. The maximum power density without TFTCs is 490 mW/cm^2 , and that with TFTCs is 470 mW/cm^2 . The difference is 4.08% , an accepted repeatability for engineering research, if total difference is attributed to the set of TFTCs.

Finally, at the same time of the fuel cell performance measurement, start and record the real-time temperature distribution measurement in the cell by the TFTCs.

Table 2
Fuel cell initial conditions.

Items	Setting values
O_2 flow rate/srpm	0.657
H_2 flow rate/srpm	0.777
Cathode backing plate temperature/ $^\circ\text{C}$	70 [28]
Anode backing plate temperature/ $^\circ\text{C}$	70 [28]
O_2 humidifier temperature/ $^\circ\text{C}$	36.7 [26]
H_2 humidifier temperature/ $^\circ\text{C}$	70 [26]
O_2 inlet temperature/ $^\circ\text{C}$	70 [26]
H_2 inlet temperature/ $^\circ\text{C}$	70 [26]

4. Results and discussion

4.1. Real-time measurement of outside temperature

As indicated above, when the fuel cell was operated under seven different constant voltages, the temperature distributions outside the cell measured by fifteen sheathed thermocouples at the back side of the ACCP were recorded. Meanwhile, the current density and cell temperature monitored by Arbin testing system were also observed. The variations of these parameters are plotted in Fig. 7, where the black line stands for the temperature variations of cell at the anode side and the red line stands for the output of current density.

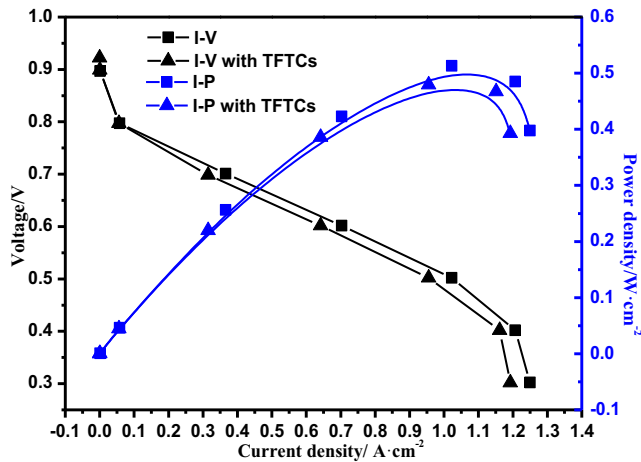


Fig. 6. Performance curve of fuel cell embedded with and without TFTCs.

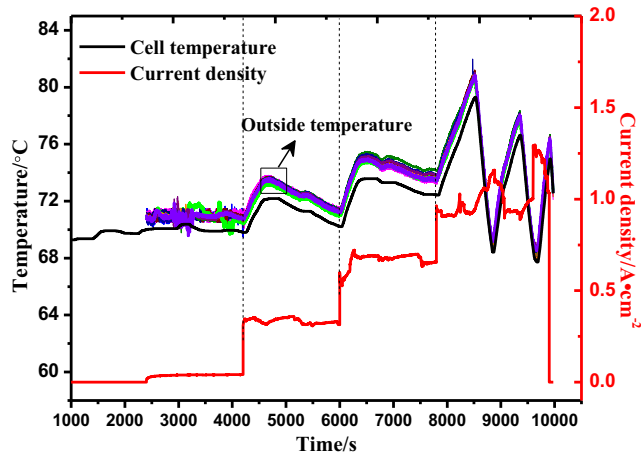


Fig. 7. Real-time measurement of outside temperature (measured by fifteen sheathed thermocouples), cell temperature at anode side and current density.

It can be seen from Fig. 7 that there exists a little temperature difference among the fifteen measuring spots of outside temperature which are free from the complex environment inside the PEMFC. It should be noted that the large temperature fluctuation in the later half test time period (see Fig. 7) is due to the opening of air forced cooling system to avoid overheated when the current density approaches 1 A/cm^2 [30]. We can find that the outside temperatures (measured by fifteen sheathed thermocouples) have the same variation trend as the cell temperature (monitored by the Arbin testing system), when response to the change of cell voltage. Because the measuring spots of outside temperature are closer to the heating rod than the measuring spot of cell temperature, the outside temperature is always higher than cell temperature. When output current density increases with the decreasing cell voltage, the response times of cell temperature and outside temperature were around 60 s and 48 s, respectively. Although the inserted sheathed thermocouples can realize the real-time temperature measurement outside the cell, they couldn't reflect the real temperature distribution inside the fuel cell with complicated environment.

4.2. Real-time measurement of inside temperature

In this section, the real-time temperature inside the PEMFC measured by the TFTCs are studied. The real-time measurement

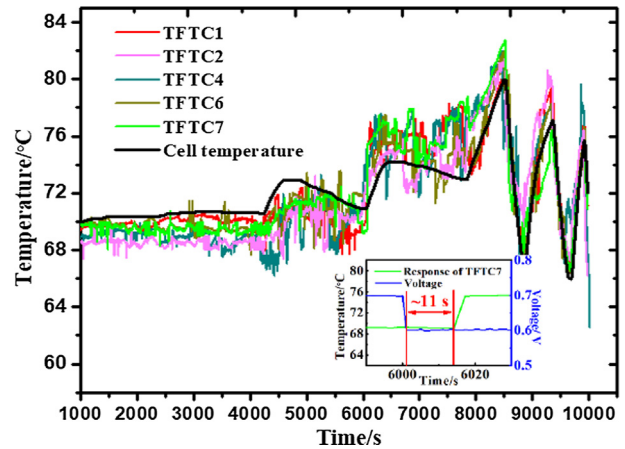


Fig. 8. Real-time measurement of inside temperature and cell temperature at cathode side.

results of the local temperature inside the fuel cell by TFTCs are shown in Fig. 8, in which the variation of cell temperature at the cathode side monitored by the Arbin testing system is also presented (black line). Generally speaking, the temperature variations measured by the TFTCs have the same trend as the cell temperature. The output current density increases with the descending voltage, thus further leading to the temperature increase. The real-time temperature variation is recorded and the moment that the temperature suddenly increases can be determined as shown in the partial enlarged detail of Fig. 8. Thus, the time delay of temperature rise in response to the voltage decrease is defined as the response time. It can be found that the representative response time of TFTC7 was about 11 s which was much faster than that of sheathed thermocouples inserted at the back side of ACCP, meaning that the TFTC can rapidly reflect the inside temperature variation. At the current density less than 0.3 A/cm^2 , the inside temperature measured by TFTCs is lower than the cell temperature. On the contrary, when the current density is more than 0.3 A/cm^2 , the TFTCs measured temperature is higher than cell temperature at the cathode side due to the drastic increase of electrochemical reaction. As shown in the Fig. 8, the temperature variation curves measured by TFTCs exist several sudden fluctuations which may be due to the appearance of condensed water in the gas diffusion layer. Because the temperature of the gas diffusion layer is lower than the catalyst layer, the water vapor could condensate at certain spots where it reaches the local saturation concentration. In the present study, the parallel flow field plate with simplest channel layout was adopted. In this flow plate, the reactant gas velocity in each channel is relatively low. When water flows pass the surface of TFTCs, the measured temperature by TFTCs can have an abrupt drop. And the washout of TFTCs by reactant gases may increase the measured temperature, leading to a zig-zag temperature variation pattern. Among the indicated five TFTCs, the variation curve of No.4 TFTC is more conspicuous. Because it was put on the bottom of flow field plate where water can be accumulated easily, resulting in a more frequent fluctuations and larger amplitude than the other TFTCs.

4.3. Inside temperature variation with voltage at five locations

To obtain temperatures of typical locations inside the PEMFC, we average the time-variation real-time temperature measured by TFTCs 1,2,4,6,7 (see Fig. 4(a)) under the voltages of 0.8 V/0.7 V/0.6 V/0.5 V. Fig. 9 presents the temperatures of the five locations at four voltages. It can be seen that the decrease of cell

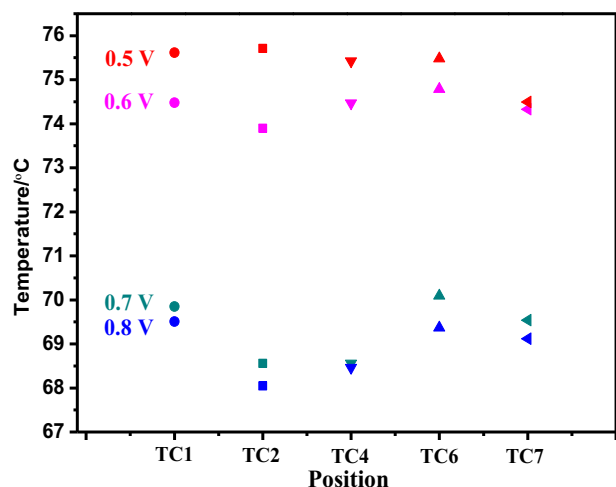


Fig. 9. Temperature distribution inside the PEMFC at different cell voltage.

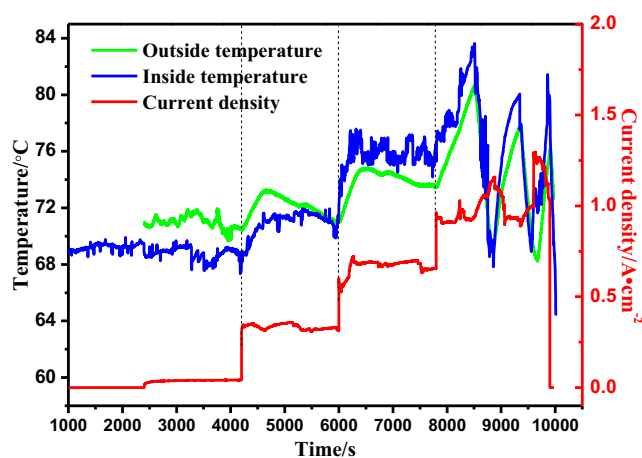


Fig. 10. Comparison of temperature variation between the outside current collector plate and inside MEA.

voltage results in the rise of temperature because of the increase of the current density.

From the performance curve (*I-V* curve) shown in Fig. 6, we can see that when the cell voltage changes from 0.7 V to 0.6 V, it corresponds to the largest rise of current density compared with other situations. As a result, the temperature difference between the 0.7 V and 0.6 V is the largest (shown in Fig. 9) since more Joule heat ($Q = I^2R$) is produced. It can also be seen from Fig. 9 that the positions closer to the entrance of flow channel (TFTCs 1 and 6) have the higher temperature. In contrast, the positions closer to the bottom of the flow field plate or closer to the exit of flow channel (TFTCs 2 and 4) have the lower temperature. This kind of the local temperature difference is consistent with the inside fuel cell multiphysics process. The embedded TFTCs have small enough spatial resolution that can recognize such detailed difference. All these maximum deviations of temperature caused by different measurement sites at the same voltage do not exceed 1.5 °C.

4.4. Comparison of outside and inside temperature variation

As indicated above, the outside temperature of PEMFC is measured by the sheathed thermocouples while the inside temperature of PEMFC is measured by the embedded TFTCs. Fig. 10 shows the comparisons of temperature variations between the outside current collector plate measured by the sheathed thermocouples and inside

MEA measured by the embedded TFTCs. Both outside plate temperature and inside temperature measured by TFTCs are the space averaged ones at any instant. From Fig. 10 following features may be noted. First, generally speaking the variation trends of both the outside and inside temperatures of the cell are in accordance with the current variation trend. Second, because of the reason mentioned above the temperatures close to MEA measured by TFTCs have a more frequent fluctuation than the outside temperature close to current collector plate. Third, the temperature of outside current collector plate is higher than that of the inside MEA when the current density is lower than 0.65 A/cm², while the temperature of MEA is equal or even superior to the outside current collector plate when the current density is over 0.65 A/cm². Such phenomenon is the consequence of the different heat flux generated in the cell. At the low current density, the heat generated by the electrochemical reaction inside the PEMFC is lower than the power of the heating rods at the end plate, which results in a higher temperature of the plate. With the increase of current density, more Joule heat will be dramatically generated, and the inside temperature appreciably increases, even surpasses the plate temperature.

5. Conclusions

In the present study, flexible Type-T thin film thermocouples (TFTCs) were fabricated based on the micro-electro-mechanical system and the manufacturing technique of embedded TFTCs was developed for real-time measurement of temperature distribution inside proton exchange membrane fuel cells. The TFTCs are fabricated on a 25 μm thick polyimide film with excellent durability, which is convenient to be inserted into the fuel cell without destruction of the original cell structure. The current TFTCs are thin enough to be placed between the membrane electrode assembly and flow field plate without causing the leakage of reactant gases and have minimal interference to the performance of the fuel cell.

The real-time temperature measuring experiment of proton exchange membrane fuel cell was carried out on an Arbin testing system. The outside temperatures at the back side of current collector plate were measured using fifteen sheathed thermocouples; while the inside temperatures on membrane electrode assembly is measured using embedded TFTCs. Following conclusions can be concluded:

- (1) For temperature distribution outside the cell, the inserted sheathed thermocouples can measure the outside temperature sensitively and there is a little temperature difference among the different measuring spots of outside temperature.
- (2) For temperature distribution inside the cell, the time-averaged temperature difference among the different positions on the membrane electrode assembly is larger than the temperature difference outside cell but not exceeds 1.5 °C at the same cell voltages. The position closer to the bottom of flow field plate the temperature will have a more frequent fluctuation.
- (3) Compared with the temperature variation of outside current collector plate, the inside temperature monitored by TFTCs has a more frequent fluctuation. The embedded TFTCs have a shorter response time to the variation of current density than the fifteen sheathed thermocouples.

Acknowledgement

This study is supported by the Key Project of National Natural Science Foundation of China (51836005), the National Key

Research and Development Program (2017YFB0102702) and the Foundation for Innovative Research Groups of the National Natural Science Foundation of China (51721004).

References

- [1] S. Sharma, B.G. Pollet, Support materials for PEMFC and DMFC electrocatalysts—A review, *J. Power Sources* 208 (2012) 96–119.
- [2] T.J. Dursch, G.J. Trigub, J.F. Liu, et al., Non-isothermal melting of ice in the gas-diffusion layer of a proton-exchange-membrane fuel cell, *Int. J. Heat Mass Transf.* 67 (2013) 896–901.
- [3] T. Murahashi, H. Kobayashi, E. Nishiyama, Combined measurement of PEMFC performance decay and water droplet distribution under low humidity and high CO, *J. Power Sources* 175 (1) (2008) 98–105.
- [4] L.M. Pant, S.K. Mitra, M. Secanell, A generalized mathematical model to study gas transport in PEMFC porous media, *Int. J. Heat Mass Transf.* 58 (1–2) (2013) 70–79.
- [5] W.Z. Fang, Y.Q. Tang, C. Ban, et al., Atomic layer deposition in porous electrodes: a pore-scale modeling study, *Chem. Eng. J.* 378 (2019) 122099.
- [6] G. Hinds, M. Stevens, J. Wilkinson, et al., Novel in situ measurements of relative humidity in a polymer electrolyte membrane fuel cell, *J. Power Sources* 186 (1) (2009) 52–57.
- [7] G. Zhang, S.G. Kandlikar, A critical review of cooling techniques in proton exchange membrane fuel cell stacks, *Int. J. Hydrogen Energy* 37 (3) (2012) 2412–2429.
- [8] S.G. Kandlikar, Z. Lu, Thermal management issues in a PEMFC stack – A brief review of current status, *Appl. Therm. Eng.* 29 (7) (2009) 1276–1280.
- [9] J.G. Pharoah, O.S. Burheim, On the temperature distribution in polymer electrolyte fuel cells, *J. Power Sources* 195 (16) (2010) 5235–5245.
- [10] W.Z. Fang, Y.Q. Tang, L. Chen, et al., Influences of the perforation on effective transport properties of gas diffusion layers, *Int. J. Heat Mass Transf.* 126 (2018) 243–255.
- [11] A. Serov, C. Kwak, Review of non-platinum anode catalysts for DMFC and PEMFC application, *Appl. Catal. B* 90 (3–4) (2009) 313–320.
- [12] H. Guo, M.H. Wang, F. Ye, et al., Experimental study of temperature distribution on anodic surface of MEA inside a PEMFC with parallel channels flow bed, *Int. J. Hydrogen Energy* 37 (17) (2012) 13155–13160.
- [13] H. Guo, M.H. Wang, J.X. Liu, et al., Temperature distribution on anodic surface of membrane electrode assembly in proton exchange membrane fuel cell with interdigitated flow bed, *J. Power Sources* 273 (2015) 775–783.
- [14] J.X. Liu, H. Guo, X.M. Yuan, et al., Effect of mode switching on the temperature and heat flux in a unitized regenerative fuel cell, *Int. J. Hydrogen Energy* (2018).
- [15] C.Y. Lee, C.H. Chen, C.Y. Chiu, et al., Application of flexible four-in-one microsensor to internal real-time monitoring of proton exchange membrane fuel cell, *Sensors* 18 (7) (2018) 2269.
- [16] C.Y. Lee, W.Y. Fan, C.P. Chang, A novel method for in-situ monitoring of local voltage, temperature and humidity distributions in fuel cells using flexible multi-functional micro sensors, *Sensors* 11 (2) (2011) 1418–1432.
- [17] C.Y. Lee, W.Y. Fan, W.J. Hsieh, In-situ monitoring of internal local temperature and voltage of proton exchange membrane fuel cells, *Sensors* 10 (7) (2010) 6395–6405.
- [18] H.Y. Wang, W.J. Yang, Y.B. Kim, Analyzing in-plane temperature distribution via a micro-temperature sensor in a unit polymer electrolyte membrane fuel cell, *Appl. Energy* 124 (2014) 148–155.
- [19] S. He, M.M. Mench, S. Tadigadapa, Thin film temperature sensor for real-time measurement of electrolyte temperature in a polymer electrolyte fuel cell, *Sens. Actuators, A* 125 (2) (2006) 170–177.
- [20] S.K. Lee, K. Ito, K. Sasaki, Temperature measurement in through-plane direction in PEFC with a fabricated in-line thermocouple and supporter, *ECS Trans.* 25 (1) (2009) 495–503.
- [21] S.T. Ali, J. Lebak, L.P. Nielsen, et al., Thin film thermocouples for in situ membrane electrode assembly temperature measurements in a polybenzimidazole-based high temperature proton exchange membrane unit cell, *J. Power Sources* 195 (15) (2010) 4835–4841.
- [22] T. Sugimoto, Y. Horiuchi, T. Araki, Developments of MEMS-based thermocouple array for sensing effects of a flow channel on PEMFC local temperature distribution, ASME 2013 11th International Conference on Nanochannels, Microchannels, and Minichannels, American Society of Mechanical Engineers, 2013.
- [23] <http://www.dupont.com/>.
- [24] D.L.D. Dowell, A critical look at type T thermocouples in low-temperature measurement applications, *Int. J. Thermophys.* 31 (8–9) (2010) 1527–1532.
- [25] H. Lin, T.F. Cao, L. Chen, et al., In situ measurement of temperature distribution within a single polymer electrolyte membrane fuel cell, *Int. J. Hydrogen Energy* 37 (16) (2012) 11871–11886.
- [26] <http://www.arbin.com>.
- [27] R. Cuccaro, M. Lucariello, A. Battaglia, et al., Research of a HySyLab internal standard procedure for single PEMFC, *Int. J. Hydrogen Energy* 33 (12) (2008) 3159–3166.
- [28] D.H. Ahmed, H.J. Sung, Effects of channel geometrical configuration and shoulder width on PEMFC performance at high current density, *J. Power Sources* 162 (1) (2006) 327–339.
- [29] K. Tajiri, C.Y. Wang, Y. Tabuchi, Water removal from a PEFC during gas purge, *Electrochim. Acta* 53 (22) (2008) 6337–6343.
- [30] J. Divisek, *Low Temperature Fuel Cells, Handbook of Fuel Cells*, John Wiley & Sons, Ltd, 2010.